

EQUULEUS Mission Analysis: Design of the Science Orbit Phase

By Kenshiro OGURI,¹⁾ Kota KAKIHARA,¹⁾ Stefano CAMPAGNOLA,²⁾ Naoya OZAKI,¹⁾
Kenta OSHIMA,³⁾ Tomohiro YAMAGUCHI,⁴⁾ and Ryu FUNASE¹⁾

¹⁾*Department of Aeronautics and Astronautics, The University of Tokyo, Tokyo, Japan*

²⁾*Jet Propulsion Laboratory, California Institute of Technology, CA, USA*

³⁾*Department of Applied Mechanics and Aerospace Engineering, Waseda University, Tokyo, Japan*

⁴⁾*Institute of Space and Astronautical Science, JAXA, Sagami-hara, Japan*

Libration point orbits, in particular those in the Earth-Moon system, have been attracting attention for science and future human space exploration. EQUULEUS is a CubeSat planned to be launched by the NASA's SLS EM-1 vehicle and aims to reach and stay around the Earth-Moon L2 point with a purpose of scientific observation. As EQUULEUS is a piggyback spacecraft with various potential launch trajectories given by the primary payload (Orion spaceship), we need to prepare a variety of science orbits with many orbit insertion epochs beforehand, which is a unique problems to piggybacked spacecraft. We have developed a systematic way to generate a large set of quasi halo orbits with estimated stationkeeping cost in a multi-body dynamics model. This paper introduces the systematic approach and shows current results of the science orbit design for EQUULEUS.

Key Words: EQUULEUS, Trajectory design, Multi-body dynamics, Halo orbit, Lagrange point, Optimization

1. Introduction

Libration point orbits, in particular those in the Earth-Moon system, have been attracting attention for science and future human space exploration. Exploring these orbits via micro spacecraft will contribute to high-frequency, low-cost visits to the cislunar space. EQUULEUS, a 6U CubeSat being developed by the University of Tokyo and JAXA, will target the second Earth-Moon Lagrange point (EML2), with purposes of engineering demonstration and scientific observation.¹⁾

Trajectory design for micro-spacecraft has two limitations to be taken into consideration: 1) given launch conditions determined by the primary payload and 2) limited delta-V capability. For the EQUULEUS, a number of possible launch trajectories and the chaotic dynamics around the libration point orbit can produce a countless number of potential orbit insertion conditions in terms not only of orbit energy but also of insertion epochs. In other words, we have to generate libration point orbits of various initiation times. Trajectory design for the transfer phase is presented in Oshima et. al.²⁾ Since the solar gravity and lunar orbit eccentricity are time-dependent and non-negligible perturbation, designing the libration point orbits with various insertion epochs needs to use a multi-body gravitational model. In addition, in light of the limited delta-V capability, fuel consumption for stationkeeping around the science orbits will be a critical factor of mission sustainability. When designing the whole trajectory by connecting transfer orbits and science ones, the stationkeeping cost should be taken into consideration. The cost would be also affected by the time-dependency of the perturbation; thus we need to estimate it in the same multi-body dynamics as in the orbit generation. Therefore, in the science orbit design, we have to prepare a pool of various potential destination orbits in a multi-body dynamics with each stationkeeping cost.

Trajectory design and stationkeeping around libration points

in the EML region have been mostly investigated along with mission analysis of the first EML libration point mission: ARTEMIS.^{3,4)} Different from the case of our mission analysis, the ARTEMIS mission did not need various libration point orbits beforehand because the spacecraft was already in orbit when designing the transfer orbits.⁵⁾ An existing approach to the quick design of libration point orbits is to prepare a catalog of the orbits made in the circular restricted three-body problem (CRTBP).^{6,7)} In the procedure, with given mission requirements, appropriate orbits in CRTBP are picked up from the catalog and converted into multi-body-dynamics ones by using the differential corrector method.⁸⁾ While this approach would be beneficial in case the designer can choose launch conditions for the selected science orbits, it cannot provide orbits of various initiation epochs because of the dynamics model the catalog is based on (i.e., not n-body dynamics but CRTBP). As for the stationkeeping analysis, several strategies have been proposed thus far, including unstable mode canceling (Floquet mode approach)⁹⁾ and target point method.¹⁰⁾ Although several studies have investigated stationkeeping cost by using these approaches,¹¹⁻¹³⁾ they do not analyze the potential time-dependency of stationkeeping cost.

This paper introduces a strategy of designing various libration point orbits in terms of size, period, and, importantly, insertion time, with stationkeeping cost in a multi-body dynamics model. The proposed method systematically computes the science orbits in a multi-body model and performs their time-continuation, which expands the orbits along the time-axis. Taking advantage of the generated orbits as reference trajectories, a computationally efficient Monte Carlo routine is devised for estimation of each stationkeeping cost. The science orbit design for EQUULEUS demonstrates the capability of the whole proposed procedure.

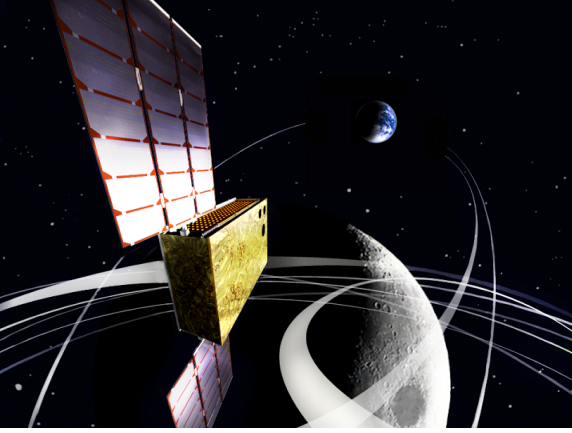


Fig. 1. A conceptual figure of EQUULEUS spacecraft.

Maneuver	LGA 2 (full success)		EML2 arrival (8-month op.)		1 month @ EML2 (extra success)		1 year @ EML2	
	DV μ [m/s]	DV σ [m/s]	DV μ [m/s]	DV σ [m/s]	DV μ [m/s]	DV σ [m/s]	DV μ [m/s]	DV σ [m/s]
DV1	10.000	0.333	10.000	0.333	10.000	0.333	10.000	0.333
Gravity Loss during DV1	1.000	0.000	1.000	0.000	1.000	0.000	1.000	0.000
TCM1+CUM1	10.000	3.333	10.000	3.333	10.000	3.333	10.000	3.333
DV2	0.200	0.000	0.200	0.000	0.200	0.000	0.200	0.000
TCM2+CUM2	5.000	1.667	5.000	1.667	5.000	1.667	5.000	1.667
DV3	0.000	0.000	8.400	0.000	8.400	0.000	8.400	0.000
TCM3+CUM3	0.000	0.000	5.000	1.667	5.000	1.667	5.000	1.667
Unloading (per year)	1.101	0.000	3.699	0.000	4.192	0.000	9.699	0.000
Station Keeping (per year)	0.000	0.000	0.000	0.000	1.644	0.000	20.000	0.000
Total DVμ [m/s]		27.3		43.3		45.4		69.3
DV μ+σ [m/s]		31.0		47.4		49.5		73.4
DV μ+3σ [m/s]		38.5		55.6		57.7		81.6

Fig. 2. Delta-V budget for the current baseline.¹⁴⁾

2. Background

2.1. EQUULEUS mission

EQUULEUS will be the first 6U CubeSat to explore the EML2, planned to be launched by NASA's Space Launch System (SLS) Exploration Mission-1 (EM1). The mission aims to demonstrate trajectory control technology in the EM region via CubeSat and to perform scientific observation assessing the flux of meteors impacting on the lunar dark side. A conceptual figure is illustrated in Fig. 1. We cannot choose the launch conditions based on our mission analysis results, as the launch trajectory of EQUULEUS is determined for the sake of the primary payload Orion vehicle.

Delta-V amount of the spacecraft is limited due to the small body. A Delta-V budget table for the current baseline trajectory is shown in Fig. 2, which indicates that the annual delta-V cost for stationkeeping is assumed 20 [m/s] when considering the balance of fuel consumption throughout the whole mission. With possible errors in orbit determination (OD), orbit insertion (OI), and maneuver execution, we need to find reasonable solutions within the limited delta-V capability.

2.2. A trajectory optimization tool: jTOP

The trajectory optimization in a multi-body dynamics model is performed by a trajectory optimization tool jTOP, which has been successfully employed in several applications including mission analysis and trajectory design for the world first deep-space micro spacecraft PROCYON.¹⁵⁾ In the process, the optimization problems are converted into forms efficiently solved by a commercial non-linear programming software SNOPT.¹⁶⁾ Our investigation exploits the optimization robustness and computational speed of the jTOP (see Ref.¹⁵⁾ for detail).

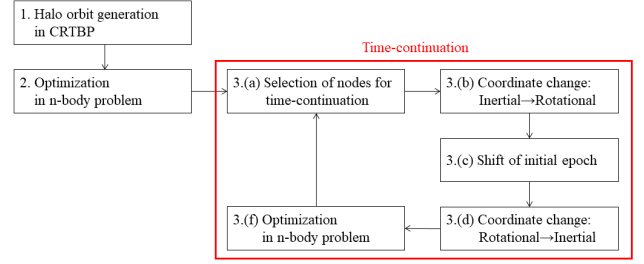


Fig. 3. Generation procedure of a family of quasi halos in n-body dynamics.

3. Quasi halo generation

This section introduces a systematic method that computes quasi-halos of various properties and initiation epochs for the preparation of the science orbits. We currently plan to choose the quasi-halo orbits around the EML2 as science orbits. The science orbit design is roughly divided into I: generation of various halo types in terms of size and shape and II: time-continuation of the halos. Each type of generated halos in the procedure I is called a family in this paper, and all these families are expanded along the time axis by the procedure II to meet the all potential orbit insertion epochs. Since the dynamical system is the time-dependent n-body problem, quasi halo orbits are time-dependent and do not have the same trajectory even in the same family.

3.1. Outline of procedure

The procedure that systematically computes a family of quasi-halos is outlined in the following as well as indicated in Fig. 3. Each procedure is detailed in the following subsections.

1. HALO GENERATION IN CRTBP

A halo in CRTBP is generated, which represents a family.

2. QUASI HALO GENERATION: CRTBP TO N-BODY DYNAMICS

The CRTBP halo orbit is optimized in the n-body problem.

3. FAMILY GENERATION: TIME CONTINUATION

- Two points per a revolution extracted as nodes from an optimized n-body quasi halo
- Coordinate change: inertial \rightarrow earth-moon rotational
- Time shift of initial epoch
- Coordinate change: earth-moon rotational \rightarrow inertial
- Optimization in n-body dynamics
- Return to 3 (a) (used as a new reference orbit)

3.2. Halo generation in CRTBP

Halo orbits in CRTBP are created by the differential corrector method shown in Howell (1984), where we choose arbitrary size and number of revolutions.⁸⁾ The size represents a family and here we use the x-position of the perilune as a representative parameter of a family. As these halo orbits are non-dimensional, dimensionalization is performed next. Two points per a revolution, both of whose y position are equal to zero (perilune and apolune), are selected as nodes for the dimensionalization and the jTOP optimizer routine. Dimensionalization and optimization are explained in the next subsection.

3.3. Quasi halo generation: CRTBP to n-body dynamics

This subsection introduces the generation procedure of the first-quasi halo orbit in n-body problem. This orbit also be-

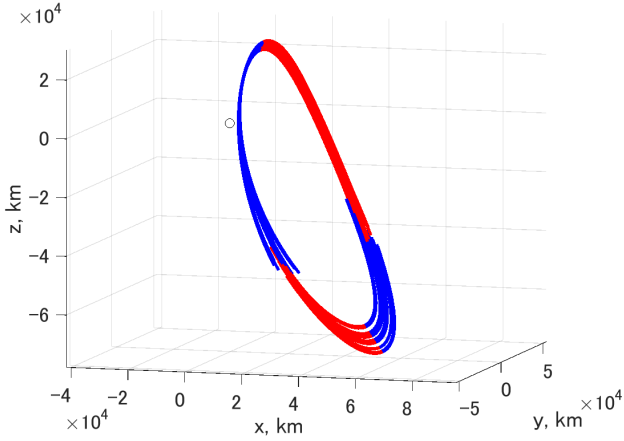


Fig. 4. A CRTBP initial guess for quasi halo orbit optimization. The blue and red lines respectively show the backward and forward propagation in the jTOP optimization.

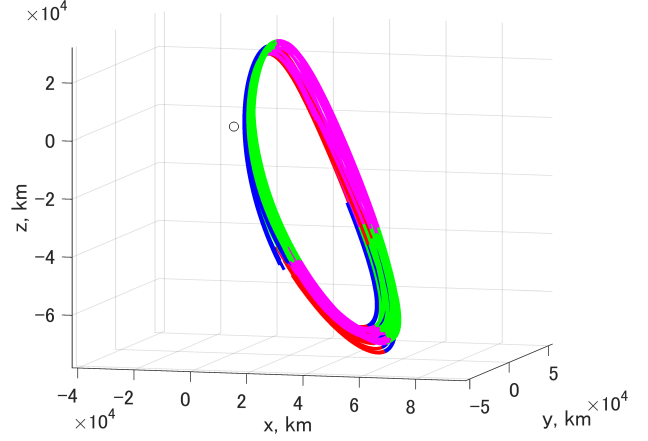


Fig. 5. A CRTBP initial guess (blue, red) and an optimized quasi halo (green, magenta). The green and magenta lines respectively show the backward and forward propagation after optimization in the jTOP.

comes the first reference orbit of the family generation. A non-dimensional CRTBP halo orbit, which is the initial guess in this procedure, is dimensionalized and optimized to become a ballistic trajectory.

3.3.1. Dimensionalization

The dimensionalization units of distance and time are respectively $l_{unit} = l_{EM}$ (the distance between the earth and the moon) and $t_{unit} = \sqrt{l_{EM}^3/\mu}$, where $\mu = G(m_E + m_M)$ is sum of the gravitational constants of the earth and the moon. It is assumed that the time between one node and the next node is the same (periodic) and it is a half period of the halo orbit dimensionalized by time unit at the time of the first node. An example figure of a dimensionalized initial guess in this procedure is shown in Fig. 4.

3.3.2. Optimization in n-body dynamics

We generate quasi halos in a n-body problem (also a reference for family generation) by optimizing initial guesses shown in the previous section by use of the jTOP. The objective function is the total delta-V along a whole orbit, which becomes zero after optimization if there exists a quasi halo orbit for the initial guess.

The optimization process imposes two kinds of constraints. The first one is that the apolune nodes are in the x-z plane in the rotational frame and their z positions are within a certain range determined by the family type. The second one is the additional constraints on both ends of the trajectory that their velocities are perpendicular to the x-z plane. These constraints maintain the quasi-halo-like trajectory before and after the both ends. Note here that the perilune nodes are not constrained, which contributes to robust convergence of the optimization.

An example figure of an optimized quasi halo orbit is shown in Fig. 5, which indicates that the initial guess made in CRTBP is accurate enough to generate a quasi halo orbit. At the same time, it can be seen from the figure that certain difference exists between n-body quasi halos and CRTBP solutions.

3.4. Family generation: time continuation

This subsection indicates a systematic way of family generation, that is, time continuation of quasi halo orbits. Member

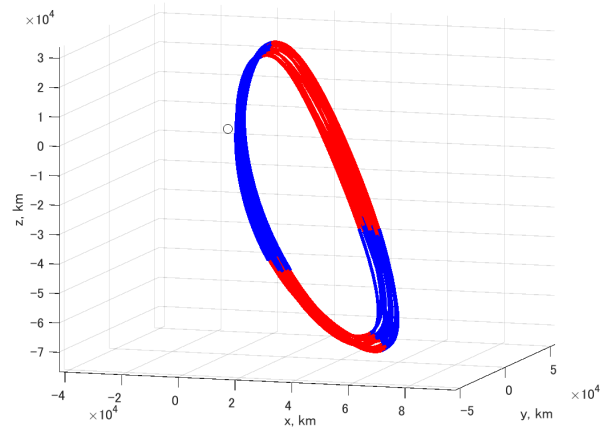


Fig. 6. An initial guess for time-continuation.

orbits of a family are repeatedly computed by optimizing initial guesses that are created by shifting the initial epoch of quasi halo orbits.

3.4.1. Shift of initial epoch

The initial guess in the procedure is generated by shifting initial epoch of a reference orbit of the family. An orbit already optimized in the previous trial is used as the reference.

Here note that the time shift should be performed in the rotational frame. Shifting the epochs of orbits in the inertial frame does not provide good initial guesses, due to the eccentricity of the lunar orbit around the earth. Thus the coordinate frame of nodes is transformed from the inertial frame to the earth-moon rotational frame. Supposing the shifting time is δt , the δt is uniformly added to the epochs of each node without any change in the positions and velocities. The time-shifted orbit is re-converted into the inertial frame, which becomes the initial guess of the family generation procedure. An example of the time-shifted quasi halo is shown in Fig. 6. This figure indicates that the initial guess in the time-continuation procedure is better than that in the single quasi-halo generation in terms of the discontinuity of the orbits (Fig. 4).

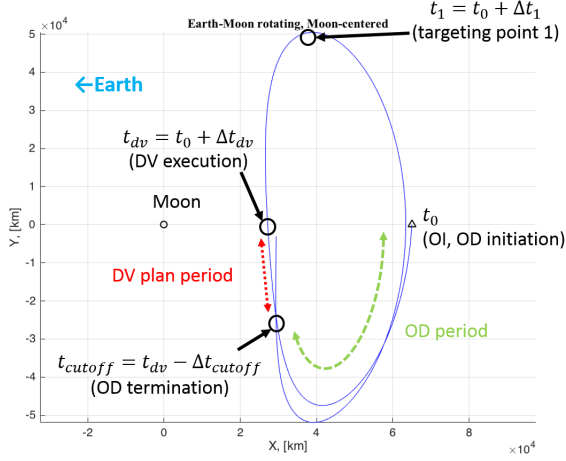


Fig. 7. Overview of stationkeeping simulation procedure

3.4.2. Optimization in n-body dynamics

Orbit optimization method in time-continuation procedure is same as that in the single quasi-halo generation. The better initial guess of the optimization allows us to optimize families of orbits (i.e., many orbits) with less computation cost and higher convergence robustness.

4. Stationkeeping analysis

This section expresses a systematic way of performing stationkeeping analysis on many generated quasi-halos in a multi-body dynamics model.

4.1. Outline

To obtain reliable stationkeeping cost estimation results, Monte-Carlo simulation of 10,000 cases is performed with respect to each reference orbit generated in the procedure in Section 3. The Monte-Carlo simulation is performed under influence of possible uncertainty of error in orbit insertion (OI) ϵ_{OI} , orbit determination (OD) ϵ_{OD} , and maneuver execution ϵ_{exec} , all of which are modeled subject to Gaussian distribution with zero mean, i.e., $\epsilon_{OI} \sim \mathcal{N}(0, \sigma_{OI}^2)$, $\epsilon_{OD} \sim \mathcal{N}(0, \sigma_{OD}^2)$, and $\epsilon_{exec} \sim \mathcal{N}(0, \sigma_{exec}^2)$. The stationkeeping maneuvers are conducted with every certain interval, namely Δt_{DV} , and every OD is terminated before each maneuver at *Cut-off* time, whose duration is termed as Δt_c (i.e., each OD duration is $\Delta t_{DV} - \Delta t_c$). In this study, the stationkeeping maneuver planning is assumed to target two downstream points ($\Delta t_1, \Delta t_2$ downstream from the OD initiation) to maintain the orbit (i.e., $M = 2$ in Eq. 5). Figure 7 illustrates an overview of the stationkeeping simulation settings.

An outline of the analysis procedure is as follows:

1. PREPARATION OF STM
Re-generate a science orbit using stacked nodes and obtain the STM computed along with the reference orbit
2. PARAMETER SETTING
Set parameters: target point Δt_i , weighting scholar R_i , and case number N
3. MONTE-CARLO SIMULATION
Run Monte-Carlo simulation shown in Algorithm 1

4. PARAMETER CHANGE AND REPEAT

Change the parameters Δt_i and R_i and repeat the procedure 3. for prescribed patterns of the two parameters

5. POST PROCESSING

Return values of the mean and standard deviation of total delta-V over the N cases for the optimal set of the parameters ($\Delta t_i, R_i$) in terms of delta-V

Through this procedure, we obtain an expected mean value of stationkeeping cost throughout a reference halo and its standard deviation with the optimal set of the parameters Δt_i and R_i in terms of delta-V.

4.2. Stationkeeping analysis algorithm

The algorithm employed in this analysis is introduced. To estimate the stationkeeping cost, this paper devises a computationally efficient Monte-Carlo simulation algorithm based on *Target Point Method* first introduced by Howell and Pernicka.¹⁰ The *Target Point Method* is summarized in Appendix A.

The constructed algorithm for the Monte-Carlo simulation is described in Algorithm 1. In the algorithm, thrust vectors for the stationkeeping maneuvers are calculated using the following equation (for derivation and detail, see Appendix. A):

$$\begin{aligned} \Delta \mathbf{V}_{plan} &= \sum_{i=1}^2 \alpha_i \mathbf{e} + \beta_i \mathbf{p}, \\ \mathbf{x}_{est}^T &= [\mathbf{p}^T, \mathbf{e}^T], \\ \alpha_i &= -[I_{3 \times 3} + R_i \mathbf{B}_{t_i, t_{DV}}^T \mathbf{B}_{t_i, t_{DV}}]^{-1} \cdot R_i \cdot \mathbf{B}_{t_i, t_{DV}}^T \mathbf{B}_{t_i, t_c}, \\ \beta_i &= -[I_{3 \times 3} + R_i \mathbf{B}_{t_i, t_{DV}}^T \mathbf{B}_{t_i, t_{DV}}]^{-1} \cdot R_i \cdot \mathbf{B}_{t_i, t_{DV}}^T \mathbf{A}_{t_i, t_c}. \end{aligned} \quad (1)$$

This algorithm computes, for a reference orbit, necessary delta-V amount for stationkeeping in N cases in terms of the random variables (ϵ_{OI} , ϵ_{OD} , and ϵ_{exec}) by one run ($N=10,000$ in this paper). Note that, in this algorithm, ϵ_{OI_j} is OI error of j -th particle ($\epsilon_{OI_j} = [\epsilon_{OI_x}, \epsilon_{OI_y}, \epsilon_{OI_z}, \epsilon_{OI_{vx}}, \epsilon_{OI_{vy}}, \epsilon_{OI_{vz}}]^T$, where $\epsilon_{OI_k} \sim \mathcal{N}(0, \sigma_{OI_k}^2)$, $k = x, y, z, vx, vy, vz$). ϵ_{OD_j} , ϵ_{exec_j} are also similarly OD error and execution error ratio of j -th particle, respectively.

Algorithm 1 Monte-Carlo for stationkeeping cost estimation

- 1: **function** SKMC($\Phi, \Delta t_{DV}, \Delta t_c, \Delta t_1, \sigma_{OI}, \sigma_{OD}, \sigma_{exec}, R, N$)
- 2: $t \leftarrow 0$
- 3: Generate $\mathcal{E}_{OI} = [\epsilon_{OI_1}, \epsilon_{OI_2}, \dots, \epsilon_{OI_N}] (\in \mathbb{R}^{6 \times N})$
- 4: OI: $\delta \mathbf{x}_{true} \leftarrow \mathcal{E}_{OI}$
- 5: **while** $t < t_{end}$ **do** $\triangleright t_{end}$: terminal time of the orbit
- 6: $t_c \leftarrow t + \Delta t_{DV} - \Delta t_c$
- 7: $\delta \mathbf{x}_{true} \leftarrow \Phi_{t_c, t} \delta \mathbf{x}_{true}$
- 8: Generate $\mathcal{E}_{OD} = [\epsilon_{OD_1}, \epsilon_{OD_2}, \dots, \epsilon_{OD_N}] (\in \mathbb{R}^{6 \times N})$
- 9: OD: $\delta \mathbf{x}_{est} \leftarrow \delta \mathbf{x}_{true} + \mathcal{E}_{OD}$
- 10: $t_1 \leftarrow t + \Delta t_1$
- 11: $t_{DV} \leftarrow t_c + \Delta t_c$
- 12: DV plan: $\Delta \mathbf{V}_{plan} \leftarrow \alpha \mathbf{e} + \beta \mathbf{p}$ (Eq. 1)
- 13: $\delta \mathbf{x}_{true} \leftarrow \Phi_{t_{DV}, t_c} \delta \mathbf{x}_{true}$
- 14: Generate $\mathcal{E}_{exec} = [\epsilon_{exec_1}, \epsilon_{exec_2}, \dots, \epsilon_{exec_N}] (\in \mathbb{R}^{3 \times N})$
- 15: $\Delta \mathbf{V}_{exec} \leftarrow \Delta \mathbf{V}_{plan} + \Delta \mathbf{V}_{plan} \odot \mathcal{E}_{exec}$ $\triangleright \odot$ represents the Hadamard product.
- 16: DV exec.: $\delta \mathbf{x}_{true} \leftarrow \delta \mathbf{x}_{true} + \Delta \mathbf{V}_{exec}$
- 17: $t \leftarrow t_{DV}$
- 18: **end while**
- 19: **end function**

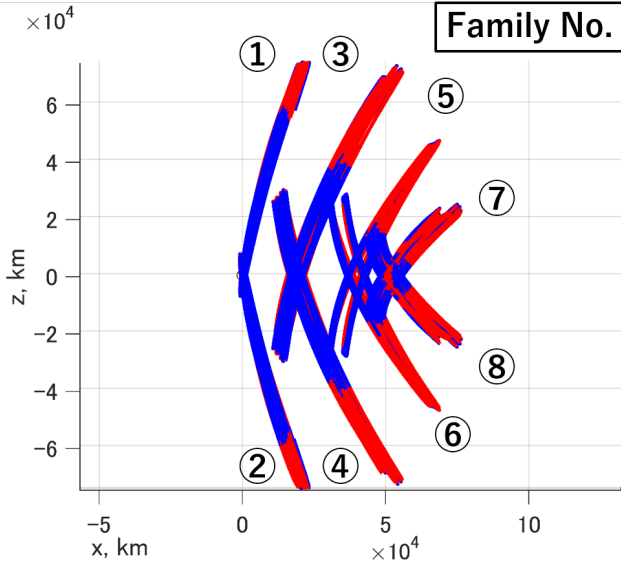


Fig. 8. Families of generated quasi halos.

5. EQUULEUS science orbit design

This section introduces current results of the science orbit design for EQUULEUS mission. In this analysis the following planets and barycenters (BCs) are considered as gravitational force sources (point masses, DE430): Sun, Earth, Moon, Mercury, Venus, Mars BC, Jupiter BC, Saturn BC, Neptune BC, and Pluto BC.

5.1. Quasi halo family database

To prepare various type properties of science orbits, we generate quasi halo orbits of 8 families shown in Fig. 8 and Table 1. Each halo's revolution number is determined so that the total duration of orbits becomes about 180 days. Fig. 8 shows that halos of large x-position have widely spread trajectories, which implies that families close to the Moon is more stable and may need less stationkeeping cost.

To be ready for various potential orbit insertion epoch, quasi-halos in each family are expanded along the time axis by time-continuation. Figure 9 illustrates the database concept and potential halo insertion epoch expected by the current transfer orbit design.²⁾ In light of unfixed launch epochs (2018/10/07 15:39 (UTC) is currently provided) and various possible insertion epochs, every halo's initial epoch is set to 6 hours interval each, ranging from 2018/09/01 0:00 to 2019/10/31 18:00, which means that 1704 orbits are prepared in each family. Note that databases are prepared in the same way with respect to each of the eight families in Fig. 8, which implies that in total 13,632 of quasi-halos are generated in the same n-body dynamics model in this case.

5.2. Stationkeeping analysis results

5.2.1. Operation constraints and errors

Here indicates the assumed values of operational constraints/conditions (Table 2) and navigation/execution errors (Table 3) in this analysis as well as those in ARTEMIS analysis.¹¹⁾ The values assumed in this analysis are preliminary ones given by other subsystems (attitude control system, propulsion system, orbit determination team, etc). The values in

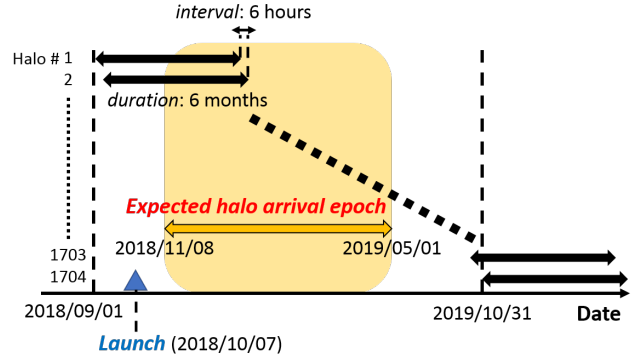


Fig. 9. Quasi halo database for science orbit design. Same databases are prepared with respect to each of families.

Table 1. Properties of generated quasi halo families

Family	x at apolune	N or S	rev. no.	rev. period [day]
1	1.040	North	23	7.6
2	1.040	South	23	7.6
3	1.120	North	14	12.3
4	1.120	South	14	12.2
5	1.160	North	12	13.6
6	1.160	South	12	13.6
7	1.177	North	12	14.1
8	1.177	South	12	14.1

ARTEMIS analysis are used to confirm the validity of the obtained cost estimation results, as it is reported that the stationkeeping cost estimation in ARTEMIS mission analysis is compatible with actual cost on orbit.¹⁷⁾

5.2.2. Baseline results

Table 4 indicates a portion of baseline results with constraints and errors of EQUULEUS case. With the assumed operational constraints and errors, stationkeeping of the families of 7 and 8 was infeasible (i.e., too large deviation occurred). As inferred in the subsection 5.1., this result indicates that the stationkeeping cost becomes worse as the x-position at the apolune of a family increases. This result implies that selecting the families of 1 ~ 4 would be better, as far as possible, in terms of fuel consumption. It should be noted that this result also implies that the assumption of impulsive thrust burn is reasonable because the amount of delta-V magnitude for one execution is less than 0.8 [m/s], which can be achieved only by an hour burn with 3 [mN] thruster planned to be installed on EQUULEUS.

Table 2. Operational constraints

Constraint	EQUULEUS	ARTEMIS
DV interval (Δt_{DV}) [day]	7.0	3.8, 7.3, 14.9, 15.2
OD cut-off (Δt_c) [day]	2.0	-

Table 3. Standard deviation of navigation/execution error

Standard deviation	EQUULEUS	ARTEMIS
$\sigma_{OD_x}, \sigma_{OD_y}, \sigma_{OD_z}$ [km]	0.47, 0.47, 1.27	1.0, 1.0, 1.0
$\sigma_{OD_{vx}}, \sigma_{OD_{vy}}, \sigma_{OD_{vz}}$ [cm/s]	0.87, 1.07, 1.80	1.0, 1.0, 1.0
$\sigma_{OI_x}, \sigma_{OI_y}, \sigma_{OI_z}$ [km]	0.47, 0.47, 1.27	1.0, 1.0, 1.0
$\sigma_{OI_{vx}}, \sigma_{OI_{vy}}, \sigma_{OI_{vz}}$ [cm/s]	0.87, 1.07, 1.80	1.0, 1.0, 1.0
$\sigma_{exec_x}, \sigma_{exec_y}, \sigma_{exec_z}$ [-]	5%, 5%, 5%	1%, 1%, 1%

Table 4. Baseline results of stationkeeping cost (Halo initial epoch: 2018/12/31)

Family	Mean annual DV [m/s]	Std. dev. of annual DV [m/s]
1	12.65	4.00
2	13.35	4.78
3	14.60	2.32
4	14.62	2.32
5	28.80	7.33
6	29.00	7.82
7	-	-
8	-	-

Table 5. Results of stationkeeping cost with ARTEMIS condition (Halo initial epoch: 2018/12/31)

Family	Mean annual DV [m/s]	Std. dev. of annual DV [m/s]
1	11.15	3.60
2	11.34	3.84
3	11.40	1.66
4	11.41	1.66
5	18.65	2.27
6	18.54	2.25
7	32.06	4.05
8	32.12	4.04

Table 5 indicates a portion of baseline results with constraints and errors of ARTEMIS case. This result is compatible with that of mission analysis for the ARTEMIS,¹¹⁾ which confirms the validation of this analysis procedure.

5.2.3. Time dependence: cost comparison within a family

Taking advantage of the large pool of time-expanded halos, we can also analyze the potential time-dependency of stationkeeping cost with respect to various initiation epochs of quasi-halos. As an instance, a result of time-dependency analysis for family 1 is shown in Fig. 10. In the analysis, mean annual delta-V is computed for orbits in the same family with various initiation time, following the same procedure discussed above.

The figure clearly shows that the annual delta-V varies dependent on the initial epochs (orbit insertion time), which implies that the time-dependency of stationkeeping cost should be paid attention as well as the other factors such as size and period. The time-dependency may be due to the time-dependent perturbation caused by the solar gravity and lunar orbit eccentricity. In order to realize such cost estimation, time-expansion of quasi-halos in multi-body dynamics is indispensable, which emphasizes the importance of this work.

6. Conclusion

This paper introduced a systematic way of generating quasi-halos with stationkeeping cost estimation analysis in multi-body dynamics model. Science orbit design for EQUULEUS demonstrated its capability of computing many halos not only of various sizes or periods but also of different orbit insertion times. The stationkeeping analysis also revealed an important fact that stationkeeping cost for the libration point orbits in the EML region can have, in addition to orbits' size or period, non-negligible dependence on orbital insertion epochs, which may be due to its time-dependent dynamical structure. As EQUULEUS mission analysis, we can readily discuss various trade-

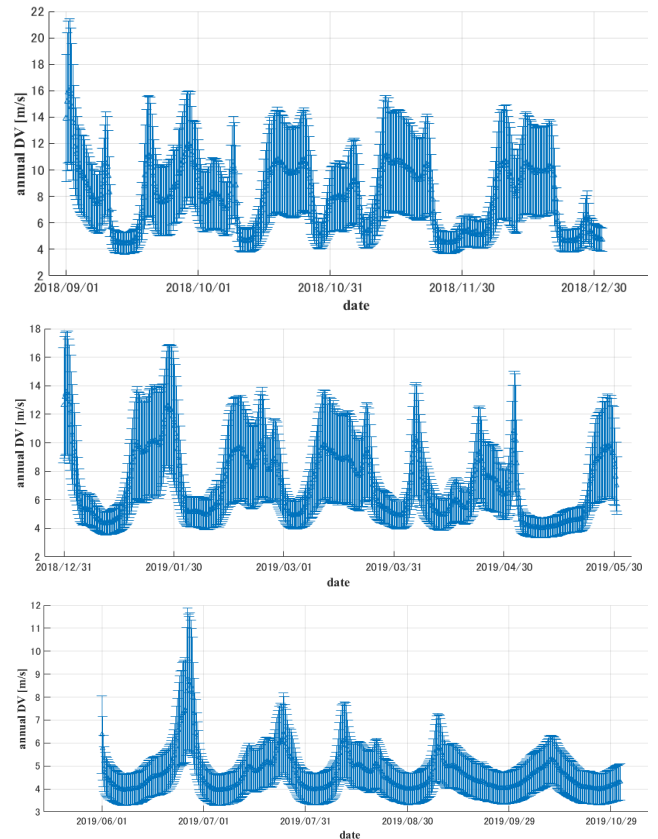


Fig. 10. Time dependence of stationkeeping cost for a Halo family 1. Horizontal and vertical axes represent quasi halo initial epoch and annual delta-V necessary for stationkeeping, respectively. Each plot shows the mean value and standard deviation of delta-V.

offs in higher levels of mission design, including stationkeeping cost and operation frequency, orbit determination frequency, and refinement of execution accuracy. The presented procedure could generally contribute to mission design of micro spacecraft to explore EML region by providing a large set of potential destination orbits with stationkeeping cost labels.

Appendix A. Target point method

The target point method algorithm provides optimal delta-V computed as a solution of linear-quadratic regulator (LQR) problem that minimizes weighted sum of magnitude of delta-V and that of position deviation from a reference orbit at a few target points downstream. By using a state transition matrix (STM) computed along with the reference trajectory, the future position deviation are approximated. Taking advantage of an analytical solution of the LQR problem, 10,000 of stationkeeping simulations are performed to evaluate the navigation and maneuver execution errors, which are assumed subject to normal distribution, with respect to several cases of weighting scalars.

Assuming the number of the target points is set to M , objective function to be minimized J is expressed as follows:

$$J = \Delta \mathbf{V}_c(t_c)^T \Delta \mathbf{V}_c(t_c) + \sum_i^M R_i \mathbf{m}_i^T \mathbf{m}_i, \quad (2)$$

where $\Delta \mathbf{V}_c(t_c)$ is trajectory correction delta-V at time t_c , R_i is a

weighting scalar with respect to the i -th target point, and \mathbf{m}_{t_i} is a predicted position deviation from a reference orbit at the i -th target point. By using STMs Φ :

$$\Phi(t_2, t_1) = \begin{bmatrix} A_{21} & B_{21} \\ C_{21} & D_{21} \end{bmatrix}, \quad (3)$$

the future prediction of the deviation can be approximated as:

$$\mathbf{m}_{t_1} \approx B_{t_1 t_0} \mathbf{e}(t_0) + B_{t_1} \Delta \mathbf{V}_c(t) + A_{t_1 t_0} \mathbf{p}(t_0) \quad (4)$$

where $\mathbf{e}(t_0)$ and $\mathbf{p}(t_0)$ are velocity and position perturbation at time t_0 , respectively. Then the LQR problem is solved and the optimal delta-V is:

$$\begin{aligned} \Delta \mathbf{V}_c(t_c) &= - \sum_i^M (\alpha_i \mathbf{e} + \beta_i \mathbf{p}), \\ \alpha_i &= [I_{3 \times 3} + R_i B_{t_i, t_c}^T B_{t_i, t_c}]^{-1} \cdot R_i B_{t_i, t_c}^T B_{t_i, t_0}, \\ \beta_i &= [I_{3 \times 3} + R_i B_{t_i, t_c}^T B_{t_i, t_c}]^{-1} \cdot R_i B_{t_i, t_c}^T A_{t_i, t_0}. \end{aligned} \quad (5)$$

References

- 1) R. Funase, N. Ozaki, S. Nakajima, K. Oguri, K. Miyoshi, S. Campagnola, H. Koizumi, Y. Kobayashi, T. Ito, T. Kudo, Y. Koshiro, S. Nomura, A. Wachi, M. Tomooka, I. Yoshikawa, H. Yano, S. Abe, and T. Hashimoto, "Mission to Earth-Moon Lagrange Point by a 6U CubeSat: EQUULEUS," in *8th Nano-Satellite Symposium*, (Ehime, Japan), 2017.
- 2) K. Oshima, S. Campagnola, C. H. Yam, Y. Kayama, Y. Kawakatsu, N. Ozaki, Q. Verspieren, K. Kakiyama, K. Oguri, and R. Funase, "EQUULEUS Mission Analysis: Design of the Transfer Orbit Phase," in *26th International Symposium on Space Flight Dynamics*, (Ehime, Japan), 2017.
- 3) V. Angelopoulos, "The ARTEMIS Mission," *Space Science Reviews*, vol. 165, no. 1-4, pp. 3–25, 2011.
- 4) T. H. Sweetser, S. B. Broschart, V. Angelopoulos, G. J. Whiffen, D. C. Folta, M. K. Chung, S. J. Hatch, and M. A. Woodard, "ARTEMIS mission design," *Space Science Reviews*, pp. 61–91, 2014.
- 5) D. C. Folta, M. Woodard, K. Howell, C. Patterson, and W. Schlei, "Applications of multi-body dynamical environments: The ARTEMIS transfer trajectory design," *Acta Astronautica*, vol. 73, pp. 237–249, 2012.
- 6) D. C. Folta, N. Bosanac, D. Guzzetti, and K. C. Howell, "An earth-moon system trajectory design reference catalog," *Acta Astronautica*, vol. 153, pp. 191–210, 2015.
- 7) D. Guzzetti, N. Bosanac, A. Haapala, K. C. Howell, and D. C. Folta, "Rapid trajectory design in the EarthMoon ephemeris system via an interactive catalog of periodic and quasi-periodic orbits," *Acta Astronautica*, vol. 126, pp. 439–455, 2016.
- 8) K. C. Howell, "Three-dimensional periodic halo orbits," *Celestial Mechanics*, vol. 32, no. 1, p. 53, 1984.
- 9) K. Howell and J. Masdemont, "Station Keeping Strategy for Translunar Libration Point Orbits," in *AAS/AIAA Space Flight Mechanics Meeting*, 1998.
- 10) K. C. Howell and H. J. Pernicka, "Station-Keeping Method for Libration Point Trajectories," *Journal of Guidance, Control, and Dynamics*, vol. 16, no. 1, pp. 151–159, 1993.
- 11) D. C. Folta, T. A. Pavlak, K. C. Howell, M. A. Woodard, and D. W. Woodfork, "Stationkeeping of Lissajous trajectories in the Earth-Moon system with applications to ARTEMIS," *Advances in the Astronautical Sciences*, vol. 136, pp. 193–208, 2010.
- 12) T. A. Pavlak, *Trajectory Design and Orbit Maintenance Strategies in Multi-Body Dynamical Regimes*. Ph.d. thesis, Purdue University, 2013.
- 13) D. C. Folta, T. A. Pavlak, A. F. Haapala, K. C. Howell, and M. A. Woodard, "Earth-Moon libration point orbit stationkeeping: Theory, modeling, and operations," *Acta Astronautica*, vol. 94, no. 1, pp. 421–433, 2014.
- 14) S. Campagnola, N. Ozaki, K. Oguri, Q. Verspieren, K. Kakiyama, K. Yanagida, R. Funase, H. C. Yam, L. Ferella, T. Yamaguchi, Y. Kawakatsu, and G. D. Yarnoz, "Mission Analysis for EQUULEUS, JAXA's Earth-Moon Libration Orbit CubeSat," in *67th International Astronautical Congress, IAC-16-B4.8.1*, (Guadalajara, Mexico), pp. 1–10, 2016.
- 15) S. Campagnola, N. Ozaki, Y. Sugimoto, C. H. Yam, C. Hongru, Y. Kawabata, S. Ogura, B. Sarli, Y. Kawakatsu, R. Funase, and S. Nakasuka, "Low-Thrust Trajectory Design and Operations of PROCYON, The First Deep-space Micro-spacecraft," in *25th International Symposium on Space Flight Dynamics*, no. 1, pp. 1–14, 2015.
- 16) P. E. Gill, W. Murray, and M. A. Saunders, "SNOPT: An SQP Algorithm for Large-Scale Constrained Optimization," *SIAM Journal on Optimization*, vol. 12, no. 4, pp. 979–1006, 2002.
- 17) M. Bester, D. Cosgrove, S. Frey, J. Marchese, A. Burgart, M. Lewis, B. Roberts, J. Thorsness, J. McDonald, D. Pease, G. Picard, M. Eckert, and R. Dumlao, "ARTEMIS operations - Experiences and lessons learned," *IEEE Aerospace Conference Proceedings*, 2014.